

Scanner-based Granularity Measurement on a Continuous Density Wedge

*Dirk W. Hertel and Bror O. Hultgren
Polaroid Corporation
Waltham, Massachusetts*

Abstract

Minimizing granularity is a key goal when designing digital photo printing media and hardware. A granularity metric that correlates well with visually perceived graininess requires measuring image noise over the entire range of image densities. We present a flatbed scanner based method of measuring granularity on a continuous (stepless) density wedge. Only one scan is necessary to provide granularity as a function of density, and hence visually weighted graininess. Digital filtering separates the spatial micro-density variation from the continuous change of density before calculating noise power spectra as a function of density with high density resolution, higher than obtainable from a step wedge target. The method has been developed into an efficient and powerful tool for characterizing and optimizing thermal print media and hardware.

Introduction

Granularity, the objective measure of image noise in an area of uniform print density is one of the most important image quality parameters when evaluating photographic and digital photo print systems. Its minimization is a key goal when designing digital photo print hardware and media. Spatial fluctuation in micro-density can be caused by variations in both the print media and the printer hardware, and the granularity contributions from each source are cumulative.

Although granularity could be measured straightforwardly as spatial variation in microdensity, such a metric would not necessarily correlate well with the visual perception of image noise¹. Graininess is the psychovisual (subjective) response to density variation in areas of uniform print density. In complex images it is a response to the granularity in uniform areas of all densities. There are spectral, spatial, and density components in image noise. Thus graininess is correlated with a weighted average over all wavelengths of the spectral range, all visually relevant spatial frequencies, and all image densities. The appropriate weighting functions are modeled on the human visual system. The functions of photopic spectral luminous efficiency, the human contrast sensitivity $E(f)$, and the graininess sensitivity $GS(D)$ are used for spectral, spatial frequency, and density weighting.

Color filters or calibrated three- or multi-channel devices can approximate the desired visual spectral response. Image noise as a function of spatial frequency is determined by the Wiener spectrum method^{2, 3}. Since granularity depends on density, measurements must be made over the whole range of image densities. A measurement series on an array of flat fields (step wedge) is often too time-consuming for routine tests unless automated scanning systems (microdensitometers, CCD image scanners⁴) are used. For small-format photo printers there is also a trade-off between the desired number and size of density steps, and the available print area.

To bypass the disadvantages associated with step wedges, granularity metrics often rely on estimating image noise in a mid luminance gray (0.75 density). This estimate is limited to comparing materials with similar characteristics of granularity versus density, e.g. conventional photographic print materials.

The success of using CCD image scanners in measuring granularity on films⁴ suggests that high-end flatbed scanners could be used for evaluating print quality. Flatbed scanners offer a low-cost, fast, user-friendly alternative⁵ to automated microdensitometers. To fully utilize their potential, granularity versus density has to be determined in a one-step process from a single scan. The continuous density wedge, routinely used for visual print quality assessment⁶, covers the entire density range in a single target and would be ideally suited for an efficient flatbed scanner based granularity and graininess measurement.

Experimental

Measuring granularity on a continuous wedge requires separating the noise signal perceived as image grain from the gradual change of density along the wedge. Our method combines digital filtering with the Noise Power Spectrum (NPS) method to estimate granularity from short data sequences.

Print, Scan and Pre-Processing

The continuous wedge target has to be printed with a sufficiently high number of gray levels to avoid contouring. The gradient should be kept below 0.5 gray levels per print line. Fiducial lines establish the relationship between the x-

coordinate of the density ramp and input data (gray level, exposure energy).

The printed continuous wedges are scanned at 1200dpi, using linear scanner settings at 42bit grayscale resolution. The pre-processing algorithm automatically detects the orientation of the wedge, truncates the image, then flips and/or rotates the image to a position of horizontally increasing density.

Pre-processing concludes with calculating either photopic visual or monochrome cmy densities. The subsequent steps of granularity-density analysis are digital filtering, segmenting, NPS and density estimation, ending with the calculation of visually weighted graininess.

Digital Filtering

Separating the granularity signal from the wedge requires the highest spatial frequency contained in the continuous wedge $f_{w,max}$ to be lower than $f_{N,min}$, the lowest spatial frequency considered by the NPS algorithm. In other words, the segment for periodogram estimation has to be long enough to still cover the visually relevant spatial frequency range down to 0.1cycles/mm, but short enough so that within each segment the grain characteristics over density can be considered to be constant. Since the density curve of a printed continuous wedge is approximately S-shaped, it can be modeled as a quarter of a full sine wave. The principal spatial frequency of a wedge of the length L is

$$f_w = \frac{1}{4L}, \quad (1)$$

For a 4" long wedge f_w is in the order of 0.001cycles/mm, well below the lowest frequency of NPS estimation.

Segmenting

The periodogram method segments the continuous wedge, with the size of each segment determined by the scanning slit dimensions (width Δx and length h), and the length N of the data sequence used for the Fast Fourier Transform (FFT).

Horizontal and vertical segmentations are performed to analyze granularity in both directions, representing slices through the two-dimensional NPS surface.

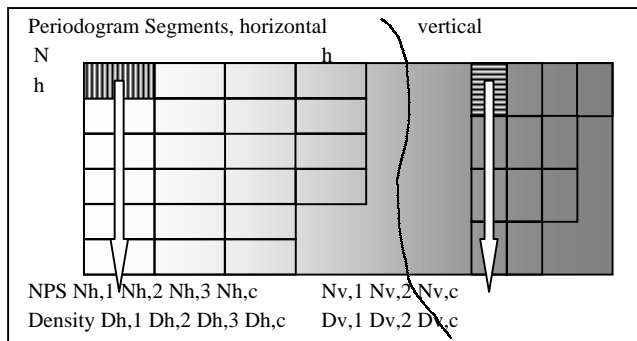


Figure 1. Scheme of segmentation for NPS measurement.

The segmentation creates sampling matrices where the number of columns and lines depend on the image size, and the size and orientation of the segments. The number of mean density levels is equivalent to the number of columns, and the number of periodograms per density level equivalent to the number of lines. The minimum number of lines and columns is set to ensure good density resolution and acceptable standard error of NPS. For small print formats segments are allowed to overlap.

Noise Power Spectrum

The segmenting is applied to both the unfiltered and the filtered images.

From the unfiltered image, density as a function of column centroid position $D(x)$ is calculated as average over all line segments.

The density fluctuation ΔD_n for each segment is calculated from the high-passed image. Pixel merging simulates horizontally or vertically oriented slit scans. For the flatbed scanner the minimum slit width is given by the pixel pitch at the optical resolution, e.g. $\Delta x = 0.021\text{mm}$ at 1200dpi. Aliasing is not a problem because the effective minimum slit width has been measured at about twice the pixel pitch.

Periodograms are calculated for each segment. The periodogram for a horizontal segment of N elements at column c and line l is

$$NPS_{c,l}^H(f_k) = \left| \sum_{n=0}^{N-1} \Delta D_n^H e^{-2\pi i k n / N} \right|^2, \quad (2a)$$

and for a vertical oriented segment it becomes

$$NPS_{c,l}^V(f_k) = \left| \sum_{n=0}^{N-1} \Delta D_n^V e^{-2\pi i k n / N} \right|^2. \quad (2b)$$

The NPS for each column c is calculated as an average of all line periodograms $N_{c,l}(f_k)$

$$NPS_c^H(f_k) = \frac{a}{LN} \sum_{l=0}^{L-1} N_{c,l}^H(f_k) \quad (3a)$$

and

$$NPS_c^V(f_k) = \frac{a}{LN} \sum_{l=0}^{L-1} N_{c,l}^V(f_k), \quad (3b)$$

where L is the number of segments per column.

The centers x of each matrix column segment correspond with exposure or energy $E(x)$. The knowledge of $E(x)$ allows the column densities D_c and $NPS_c(f, D)$ to be plotted versus energy.

Granularity and Graininess Analysis

Further steps are the integration of $NPS(f, D)$ firstly in relation to spatial frequency to calculate granularity for each density, and then in relation to density to calculate graininess from the granularity-density curve.

Granularity represents a weighted average over the spatial frequency component, using a Gaussian low pass filter formed from the spatial frequency response of the human visual system⁷ $E(f)$ for viewing reflection prints at a "normal viewing distance" of 40cm:

$$\sigma^2(D) = \frac{\int \left(\frac{E(f)}{f} \right)^2 NPS(f, D) df}{A \cdot \int \left(\frac{E(f)}{f} \right)^2 df} \quad (4)$$

The eye weighting function can be considered to be equivalent to a Gaussian weighted aperture A with a width of $560\mu\text{m}$, projected onto the image. A granularity coefficient $g(D)$ was introduced to achieve manageable granularity numbers. The relationship between $g(D)$, the standard deviation $\sigma(D)$ of density measured with an aperture area A , and the scale value of the NPS at a spatial frequency of 1cycles/mm are approximately

$$g(D) = 10^3 \cdot \sigma(D) \sqrt{A} \approx 10^3 \sqrt{N(1 \cdot \text{cycle/mm}, D)}. \quad (5)$$

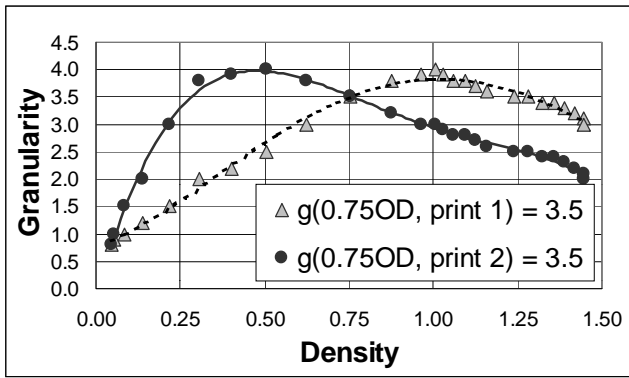


Figure 2. Density versus granularity for digital prints on (1) photographic and (2) halftone thermal media.

Granularity comparisons are made in the context of their impact on image quality. The mid-tone (0.75OD) gray granularity is often used, being based upon the density distribution of grain seen in film-like imaging systems. However, these comparisons are only valid for systems whose granularity density relationship is similar to that of photographic systems. Fig. 2 shows the density dependence of print granularity for two digital prints on (1) photographic and (2) halftone thermal media. Both prints have exactly the same midtone granularity of $g(0.75\text{OD}) = 3.5$, and about the same peak granularities, but the granularity of the thermal print peaks at much lower density of about $D = 0.5$.

The graininess metric reflects these different granularity versus density characteristics. Since the continuous wedge method delivers granularity versus density, the measured mid tone granularity can be corrected for those density distributions of granularity that are not

film-like. This is achieved by weighting the granularity at densities other than 0.75 by the graininess sensitivity function, and determining the appropriate correction factor for the granularity.

Graininess as a psychovisual response can be metricized applying established psychovisual scaling techniques such as category scaling⁸. This is based on Thurston's Law of Categorical Judgements. It is well known⁹ that the category scaled psychometric of graininess is related to granularity by:

$$G \propto \log \sigma^2 \quad (6)$$

For samples of varying density Bartleson generalizes this expression for Graininess:

$$G_{cat}(\sigma(D), D) \propto \log(GS(D) \cdot \sigma^2(D)) \quad (7)$$

where $GS(D)$ is a density-dependent weighting function determined to satisfy how graininess appears at different densities. Graininess sensitivity was originally determined from the category scaling of a series of flat fields with varying density and granularity

$$GS(D) = 10^{B(D)/C} \quad (8)$$

where

$$B(D)/C = 0.880 - 0.736 \cdot D - 0.003 \cdot D^{7.6}$$

which is in agreement with the functional form determined from results obtained by Bartleson over the common density range.

The psychometric metrics for image quality are based on grain simulations whereby grain is propagated through a film-like tone reproduction, and parameterized by the mid-tone (0.75OD) gray granularity. For imaging systems with differing density dependent granularity, the film like mid-tone (0.75OD) gray granularity must be corrected for the density dependence as weighted by the graininess sensitivity

$$\sigma_e^2 = \sigma^2(0.75) \cdot f(GS(D), \sigma^2(D))$$

$$f(GS(D), \sigma^2(D)) = \frac{\int GS_n(D) \cdot \sigma_n^2(D) dD}{\int GS_n(D) \cdot \sigma_n^2(D) |_{film} dD} \quad (9)$$

where $(\cdot)_n$ denotes normalization of the function to its value at 0.75OD. The result of the correction is visually weighted graininess

$$G = 10^3 \cdot \sigma_e \sqrt{A}. \quad (10)$$

Figure 3 shows how the density distribution of print 2 in Fig. 2 differs from the film-like characteristics, with the low-density peak of granularity receiving a higher weight than the high-density peak of print 1. At 4.3 the graininess of the thermal print 2 is considerably higher than that of the photographic print 1, where the difference between $g(0.75\text{OD}) = 3.5$ and $G(\text{print 1}) = 3.4$ is small.

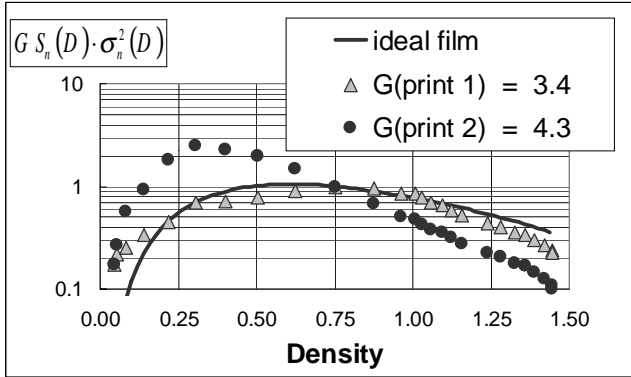


Figure 3. Distributions of $GS(D) \cdot \sigma_n^2$ for the two granularity versus density distributions from Fig. 2.

Differences between horizontal and vertical granularities indicate the presence of non-isotropic noise components such as streaking and banding.¹⁰

The analysis continues by using look-up tables to match the coordinates of the continuous wedge with exposure energy data, delivering density, slope of the density-energy curve, and granularity as functions of energy.

Results

The continuous wedge method is highly efficient, but also precise and robust because visual weighting over density minimizes the effect of outliers from localized print defects on graininess. The scanner tool has become pivotal in the design and optimization of thermal print media and hardware. Routine applications include screening media (donor, receiver), selecting hardware components (e.g. printheads), studying media-hardware interaction, and optimizing printing conditions (e.g. halftone screen, print speed, voltage).

For example, two halftone screen patterns were studied on a photographic quality direct thermal print material. Fig. 4 shows on the left a 45° pattern where each printhead element prints a dot only every other print line in alternating fashion, and on the right a rectangular pattern where each printhead element prints one dot per print line.

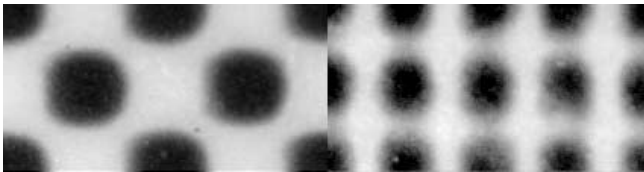


Figure 4. Dot pattern on direct thermal media: 45° (left) versus rectangular (right).

The 45° screen has half the number of dots per area, but the dots grow to twice the size at maximum density. Intuitively, smaller dots should be advantageous for better image quality, but the print with the finer screen looks more grainy, $G(\text{rect}) = 4.9$ is measured, compared to $G(45^\circ) = 3.2$. The granularity versus density curves in Fig. 5(a) show that the granularity is higher in the regions of the low- and mid-density.

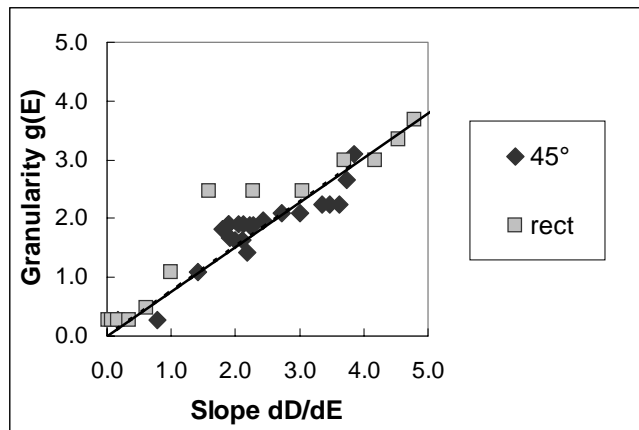
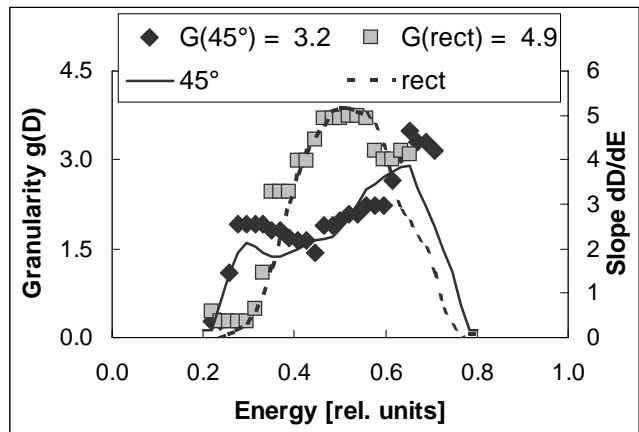
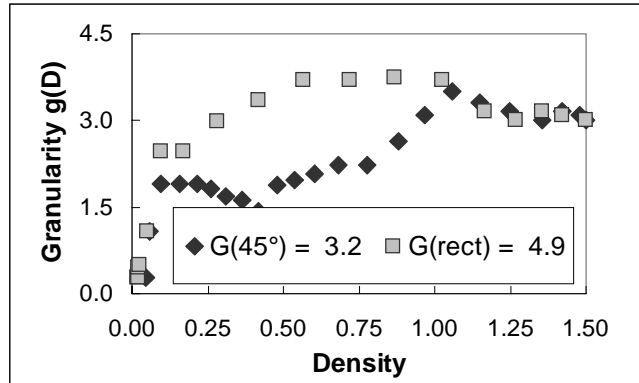


Figure 5. Thermal media printed with the two different screens: (a) Granularity versus density, (b) Granularity and slope versus energy, (c) correlation of slope and granularity.

Figure 5(b) shows the slope dD/dE of the density curve and granularity g , both plotted over print energy. When comparing the slope over energy curves it becomes apparent that with the finer screen more energy is needed to print the minimum density, but less energy to reach maximum density.

The strong correlation between granularity and slope observed in Fig. 5(c) is a recurring feature of halftone thermal print systems. The correlation coefficient can be described as a 'grain amplification factor' and is a characteristic for any given hardware-media combination.

The experiment shows the tradeoff between halftone screen resolution and granularity noise. With a finer screen, each density is composed of a larger number of smaller dots. The main contributor to granularity is the relative variation of dot size dr/r . Since the absolute dot size variation dr for any given dot size r results from media variations, and not on the choice of screens, a transition to the rectangular screen with its smaller dots will increase granularity.

An important question when modeling thermal print systems is the minimum energy necessary to produce the smallest reliable dot size. Dots should be reliably produced from an threshold energy E_{min} where the total density $D(E_{min})$ is higher than the density variation $\sigma_D(E_{min})$, or the relative granularity is below a threshold Γ

$$\frac{\sigma_D(E_{min})}{D(E_{min})} < \Gamma . \quad (11)$$

The lower the density variation for a given energy the higher the likelihood that stable dots are formed.

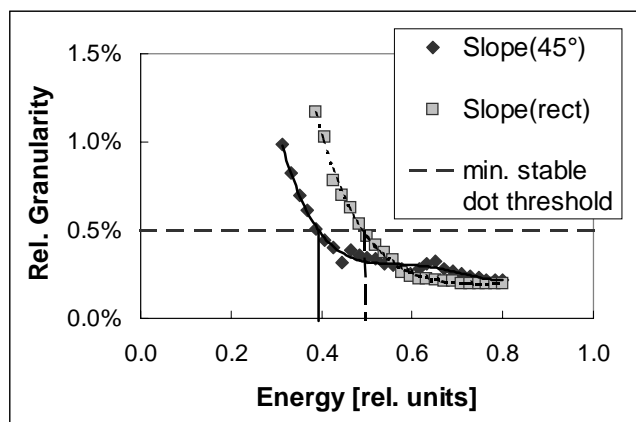


Figure 6. Relative granularity σ_D/D , threshold and energies for minimum stable dot.

For a relative granularity threshold of $\Gamma = 0.5\%$, the rectangular dot pattern requires minimum reliable dot energy a 1.28 times higher than the 45° pattern.

In summary, a tradeoff between graininess and dot visibility is observed. Printing with a finer halftone screen,

although desirable to reduce dot visibility, resulted in higher granularity, especially at low- and midtone densities. The halftone pattern with larger dots was more robust to variations due to media and hardware.

Conclusion

A scanner-based method is described that measures the entire granularity versus density characteristic for digital photo print systems using a single continuous density wedge. The granularity – graininess metric incorporates the contrast sensitivity and graininess sensitivity functions. The analysis of granularity and density as functions of energy reveals close correlation between the slope of the density curve and granularity. The energy required to print a minimum stable dot size is derived. This efficient and robust method has become an indispensable tool when optimizing thermal print media and hardware.

References

1. C. J. Bartleson, Predicting Graininess from Granularity. *J. Photogr. Sci.* **33**, 117 (1985).
2. J. C. Dainty and R. Shaw, *Image Science*, Academic Press, New York, 1974, pg. 276.
3. D. Hertel and T. Riemer, On the Measurement of Granularity and Noise Power Spectrum of Photographic Materials, *Proc. IS&T's 47th Annual Conf./ ICPS 94*, pg. 425. (1994).
4. D. Hertel, K. Töpfer, and H. Böttcher, Image Quality Investigations by Means of Photodetector Arrays, *J. Imaging Sci.* **38**, 44 (1994).
5. R. Rasmussen, B. Mishra, and M. Mongeon, Using Drum and Flatbed Scanners for Color Image Quality Measurements, *Proc. PICS*, pg. 108 (2000).
6. T. Olson, Smooth Ramps: Walking the Straight and Narrow Path through Color Space, *Proc. IS&T Seventh Color Imaging Conference*, pg. 57 (1999).
7. T. N. Cornsweet, *Visual Perception*, Academic Press (1971).
8. J. Bowman, J. Bullitt, F. R. Cottrell, and B. O. Hultgren, Color Print Image Quality, *Proc. IS&T 42nd Annual Conf.*, pg. 465. (1989)
9. C. J. Bartleson, *Optical Radiation Measurements*, Vol. 5, Chapter 8, Academic Press, New York, 1984.
10. P. J. Kane, T. F. Bouk, P. D. Burns, and A. D. Thompson, Quantification of Banding, Streaking and Grain in Flat Field Images, *Proc. PICS*, pg. 79. (2000).

Biographies

Dirk Hertel gained his physics degree (1979), and a Ph.D. (1989) for research work on the measurement and interpretation of microfilm image quality from the Technical University Dresden (Germany). He worked at the TU Dresden as assistant lecturer in imaging science, and researcher specializing in computer modeling and the microdensitometry of photographic image quality. Since joining Polaroid Corporation in 1998 he has developed scanner-based print evaluation tools and worked on

optimizing image quality in digital print media and hardware.

Bror Hultgren received his B.S. degree in Aeronautical Eng. from M.I.T. in 1962 and a Ph.D. in Physics from Boston University in 1975. Since 1979 he has worked in the Research Division of Polaroid Corporation. Currently he is

a Distinguished Scientist specializing in Image Science. During his career he has focused on developing and applying psychovisual metrics to system design and to automated image processing algorithms. In addition he has developed models of micro image structure and color reproduction in both photographic films and halftone imaging systems.